

1 **Groundwater Ages in Intertill and Buried Valley Aquifers in Saskatchewan, Canada**

2 Chandler Noyes^{1,2}, Jennifer C. McIntosh^{1,3}, Nicholas Dutka³, Rebecca Tyne⁴, Matthew B.J.
3 Lindsay⁵, and Grant Ferguson^{1,3*}

4 1. Department of Hydrology and Atmospheric Sciences, University of Arizona, Tucson, AZ,
5 USA

6 2. Waite-Heindel Environmental Management, Burlington, VT

7 3. Department of Civil, Geological, and Environmental Engineering, University of
8 Saskatchewan, Saskatoon, SK, Canada

9 4. Woods Hole Oceanographic Institution, Woods Hole, MA

10 5. Department of Geological Sciences, University of Saskatchewan, Saskatoon, SK, Canada

11 *Corresponding Author: grant.ferguson@usask.ca

12 **Abstract**

13 paleohydrogeology, glacial terrain, stable isotopes, radiogenic isotopes, dating techniques

14 **Article Impact Statement**

15 Shallow confined aquifers in Saskatchewan, Canada were recharged over a spectrum of times
16 from late Pleistocene to present.

17 **ABSTRACT**

18 Continental glaciations during the Pleistocene Epoch created complex systems of aquifers and
19 aquitards across many northern regions of the Earth. The low hydraulic conductivities of glacial
20 till aquitards suggest that limited recharge will reach the underlying aquifers, potentially

21 preserving old groundwaters. Here, we characterize the recharge history in intertill and buried
22 valley aquifers in Saskatchewan, Canada using ^{14}C , ^3H , ^4He $\delta^2\text{H}$, $\delta^{18}\text{O}$ and major ions. Intertill
23 aquifers with depths of <30 m had corrected ^{14}C ages ranging from 0 to 15.5 ka. These aquifers
24 also contained ^3H and/or elevated NO_3 in some locations, indicating that a component of modern
25 recharge had mixed with older water. A single sample from the Judith River bedrock aquifer in
26 the region had a corrected ^{14}C age of 10.2 ka and elevated NO_3 . Samples from buried valley
27 aquifers with depths of 89 to 123 m contained older waters with ages >38 ka in some locations,
28 indicating that recharge occurred before the last glacial advance over the region . While measuring
29 tracers that cover a wide range of ages is necessary to understand these flow systems, $\delta^2\text{H}$ and $\delta^{18}\text{O}$
30 were less diagnostic because values of modern winter precipitation overlapped with groundwaters
31 with a wide range of ages. The range of ages present in the intertill aquifers of the region indicate
32 that these systems are currently being recharged, which indicates some development of
33 groundwater resources is possible but also points to a need for groundwater protection measures.

34 **INTRODUCTION**

35 The bulk of the Earth's fresh groundwater is fossil (>12,000 years old) (Gleeson et al.
36 2016) and there has been debate about how strongly these waters are connected to the rest of the
37 hydrologic cycle (Bierkens and Wada 2019; Cuthbert et al. 2023; Edmunds 2003; Ferguson et al.
38 2020; Margat et al. 2006). During Pleistocene glaciations, low permeability sediments (aquitards)
39 were deposited in many regions, restricting the amount of recharge reaching underlying aquifers
40 (Hendry et al. 2005; Ferris et al. 2020; Keller et al. 1988; van der Kamp 2001; Rodvang and
41 Simpkins 2001; Gerber and Howard 1996). Glaciated areas also experienced large shifts in
42 hydrologic boundary conditions with the advance and retreat of continental ice sheets (Lemieux et
43 al. 2008; Person et al. 2007). Fossil groundwaters have been identified in various glaciated areas

44 of the northern hemisphere (McIntosh et al. 2012; Person et al. 2007), including in relatively
45 shallow aquifers in the Canadian Prairies (Grasby et al. 2000; Grasby and Chen 2005; Ruff et al.
46 2023; Grasby and Betcher 2002). The degree of isolation and potential for mixing with more recent
47 recharge has been challenged recently by the widespread presence of both fossil and modern
48 components in groundwaters in various locations globally (Jasechko et al. 2017). Here, we
49 examine the ages of groundwaters in intertill and buried valley aquifers in Saskatchewan to
50 improve our understanding of their connections to the rest of the hydrologic cycle.

51 There have been extensive efforts to understand the hydrostratigraphy of Pleistocene
52 sediments in Saskatchewan (Christiansen 1992; MDH Engineered Solutions Ltd. 2011; Maathuis
53 et al. 2011; Cummings et al. 2012) but understanding of groundwater flow patterns is limited due
54 to the discontinuous nature of these aquifers and sparse spatial coverage of observation wells.
55 Aside from the Dalmeny aquifer (Fortin et al. 1991), potentiometric surfaces have not been
56 mapped at regional or subregional scales although there have been inferences made on flow
57 directions and sources of recharge for individual wells in the SWSA observation well network
58 (Meneley et al. 1979; Saskatchewan Water Security Agency 2024a). Modern recharge is thought
59 to primarily occur through wetlands (Hayashi et al. 1998; Bam et al. 2020). Whether this recharge
60 results in a substantial flux of water to intertill aquifers and buried valley aquifers is an open
61 question, due to the low hydraulic conductivity of overlying unoxidized tills (Ferris et al. 2020).
62 These tills contain water that has been interpreted as Pleistocene in age in many locations (Keller
63 et al. 1988; Hendry et al. 2005; Hendry and Wassenaar 2011). The strength of the connection
64 between aquifers confined by till aquitards and the rest of the hydrologic cycle remains unclear
65 (Bam et al. 2020).

66 The presence of Pleistocene groundwaters in western Canada has often been identified with
67 water stable isotopes, inferring that $\delta^2\text{H}$ and $\delta^{18}\text{O}$ values that plot along the global meteoric water
68 line (GMWL), but are lower than modern precipitation or those in shallow or upgradient
69 groundwater, originated as recharge from glacial sources (Ferguson et al. 2007; Ferguson and
70 Jasechko 2015; Grasby et al. 2000; Grasby and Betcher 2002; Grasby and Chen 2005; Hendry et
71 al. 2013). However, the use of $\delta^2\text{H}$ and $\delta^{18}\text{O}$ values to identify Pleistocene recharge could be
72 complicated in some situations by overlap with older groundwater components with similar values
73 that were recharged during interglacial periods (McIntosh et al. 2012; North Greenland Ice Core
74 Project members 2004). $\delta^2\text{H}$ and $\delta^{18}\text{O}$ values may also provide inconclusive evidence of
75 Pleistocene recharge in areas, such as Saskatchewan, where isotopically-depleted snowmelt forms
76 a substantial portion of groundwater recharge (Bam and Ireson 2019; Hayashi et al. 1998).
77 Seasonal weighted average $\delta^{18}\text{O}$ values of snow in the Saskatoon region vary between -23.1 and -
78 19.7‰ (Koehler 2019), which is similar to the range of values that have been interpreted as glacial
79 in origin in western Canada of -17 to -24‰ (Ferguson and Jasechko 2015; Grasby et al. 2000;
80 Hendry et al. 2013; Ferguson et al. 2007). These $\delta^{18}\text{O}$ values overlap with the values of -15.5 to -
81 19‰ that are found in shallow groundwater in Saskatchewan (Clark and Fritz 1997; Keller et al.
82 1988; Hendry et al. 2004; Hendry and Wassenaar 1999; Bam et al. 2020; McMonagle 1987),
83 complicating interpretation of the timing of recharge. Variability in the water stable isotope values
84 of modern recharge is largely attributable to seasonality rather than elevation of recharge areas,
85 which likely varies by less than 100 m in the study area.

86 Uncorrected measurements of ^{14}C in groundwaters from glacial tills in Saskatchewan
87 indicate recharge at 22.5 to 13.3 ka at the Warman site (Keller et al. 1988) and 31 to 25 ka at the
88 King Site (Wassenaar and Hendry 2000), approximately corresponding to the LGM (Christiansen

89 1979; Dalton et al. 2022). Similar dates were estimated from ^4He concentrations in the Battleford
90 Formation tills using transient diffusion models (Hendry et al. 2005). Numerical modeling of
91 diffusion into shales from regional bedrock aquifers in the region suggest the presence of older
92 groundwaters, perhaps as old as 300 ka (Hendry et al. 2013; Mowat et al. 2021). The behavior and
93 sources of groundwater in Saskatchewan's intertill and buried valley aquifers throughout the
94 Pleistocene and Holocene is less well-constrained. Here, we analyzed multiple age tracers (^3H ,
95 ^{14}C , and ^4He), noble gases, and water stable isotopes ($\delta^{18}\text{O}$ and $\delta^2\text{H}$) of groundwater from
96 Saskatoon Group intertill and Empress Group buried valley aquifers in Saskatchewan, Canada
97 (Figure 1a). Results provide key insights into the distribution of groundwater ages in glaciated
98 regions.

99 **STUDY AREA**

100 The Köppen-Geiger climate classification of the Saskatoon Region is a cold semi-arid type,
101 typically featuring warm and dry summers with cold and dry winters (Peel et al. 2007). The
102 Saskatoon region receives an average of 347 mm of precipitation annually (Environment and
103 Climate Change Canada 2024). The majority of precipitation occurs during the late spring to early
104 summer months, while approximately one-third of precipitation falls as snow during the winter
105 months. Mean annual gross evaporation for the region, based on a 30-year period for the Canadian
106 Prairies, ranges from 800–920 mm (Martin 2002), vastly exceeding precipitation amounts. The
107 mean annual temperature is 2.4 °C and ranges from a mean monthly low of -17.5 °C in January to
108 a mean monthly high of 19.0 °C in July (Environment and Climate Change Canada 2024). The
109 Prairies are susceptible to drought conditions, having experienced many severe droughts over the
110 past 500–1,000 years (Case and MacDonald 2003)

111 Saskatchewan has experienced eight to ten periods of substantial glacial advance and
112 retreat over the past two million years, with the final glacial retreat between 17 ka to 10 ka
113 (Christiansen 1979). These cycles of deposition and erosion produced a complex sequence of
114 glacial till aquitards interlayered with sand and gravel aquifers (MDH Engineered Solutions Ltd.
115 2011). The lateral continuity of these strata is poorly understood in many cases, especially in terms
116 of their hydraulic properties (Maathuis 2005; MDH Engineered Solutions Ltd. 2011).

117 The glacial and bedrock formations of interest are the Upper Cretaceous Lea Park, Judith
118 River, and Bearpaw formations; the Empress Group (“buried valley aquifers”), which straddles
119 the Neogene-Quaternary boundary; and the Quaternary, Sutherland, and Saskatoon groups
120 (Figure 2). The Upper Cretaceous formations are generally non-calcareous shales of varying
121 marine clay, silt, and sand content, which are spatially variant due to erosion (Dawson et al. 1994;
122 McLean 1971). The Tyner and Battleford Valleys were incised into bedrock predominantly during
123 the late Neogene (Cummings et al. 2012). Substantial clastic deposits, carried by meltwater during
124 the early Pleistocene, filled these valleys in the lowlands forming the Empress Group (Cummings
125 et al. 2012; Whitaker and Christiansen 1972). The Hatfield Valley aquifer, which also contains
126 Empress Group sediments, is underlain by till locally and is thought to have been incised by
127 glaciofluvial processes during the Pleistocene (Cummings et al. 2012). Buried valley aquifers are
128 an important groundwater supply in the region and are exploited by several small municipalities
129 (MDH Engineered Solutions Ltd. 2011).

130 The overlying Sutherland Group, which was deposited prior to the Illinoian glaciation
131 (Figure 2) is divided into the Mennon, Dundurn, and Warman units. These units are further
132 subdivided into several till, intertill, and stratified units, that can be differentiated by carbonate and
133 clay content, as well as the presence of paleo-oxidized horizons and/or intertill stratified deposits

134 (Christiansen 1992; MDH Engineered Solutions Ltd. 2011). The intertill units of the Mennon,
135 Dundurn and Warman units are comprised of a range of sediment sizes from clay to gravel and
136 form discontinuous aquifers, which are not typically targets for production wells (MDH
137 Engineered Solutions Ltd. 2011).

138 The Saskatoon Group, which contains Illinoian through Late Wisconsinan-aged
139 deposits (Figure 2), is divided into the Floral and Battleford units and surficial stratified deposits.
140 The Floral and Battleford units can be differentiated from Sutherland Group units by their higher
141 carbonate content and coarser lithology, and from one another as Floral Formation sediments can
142 be delineated based upon the presence of paleo-oxidized horizons and/or intertill stratified deposits
143 (MDH Engineered Solutions Ltd. 2011). The intertill stratified deposits of the Floral Formation
144 form a discontinuous aquifer system in the region, including the Forestry Farm, Dalmeny, and
145 Tessier aquifers (MDH, 2011) (Figure 1). These aquifers are a primary target for groundwater
146 production in the region (MDH Engineered Solutions Ltd. 2011). The uppermost unit of the
147 Saskatoon Group is the surficial stratified deposits, which are postglacial sediments laid by fluvial,
148 lacustrine and aeolian processes (Christiansen 1992).

149 **METHODS**

150 **Field Methods**

151 Twelve monitoring wells were sampled June 9–17, 2022 (Figure 1). A submersible pump
152 was used to purge a sufficient volume of water from the well to satisfy US Environmental
153 Protection Agency low flow guidelines, which include stabilization of temperature, pH and
154 electrical conductivity prior to sample collection (US EPA 2017). All parameters were measured
155 using with a calibrated YSI Pro multi-parameter meter. All samples except for ^{14}C were field-
156 filtered through a 0.45 μm nylon filter into pre-cleaned sample containers. Cation, anion, trace

157 element, and alkalinity samples were collected into 30 mL high-density polyethylene (HDPE)
158 bottles with minimal headspace. Cation and trace element samples were field-acidified with ultra-
159 pure nitric acid to a pH < 2. Samples for $\delta^{18}\text{O}$ and $\delta^2\text{H}$ of water were collected into 30 mL glass
160 vials with conic tops and no headspace. ^3H was collected into 1 L HDPE bottles and carbon-13
161 ($\delta^{13}\text{C}$) of dissolved inorganic carbon (DIC) into 30 mL glass serum vials crimp sealed with no
162 headspace. Unfiltered samples were collected for ^{14}C into 1 L glass amber bottles. All samples
163 were stored on ice in the field and refrigerated in the laboratory to remain at or below 4 °C. Noble
164 gases were collected by pumping water into copper tubes, which were crimp sealed and shipped
165 to the Noble Gas Laboratory at the University of Utah (Solomon and Cook 2000).

166 **Laboratory Analysis**

167 Alkalinity analysis was performed at the University of Arizona (UARizona)'s Department
168 of Hydrology and Atmospheric Science using the Gran-Alk titration method (Gieskes and Rogers
169 1973) with an analytical precision of $\pm 0.6\%$. Anions, cations, and trace elements were quantified
170 at the Analytical Geochemistry Laboratory in the Department of Geological Sciences at the
171 University of Saskatchewan. Anions (SO_4 , Cl, F, Br, and NO_3) were measured using a Thermo
172 Dionex Integriomg HPIC system fitted with an IonPac AS11-HC-4 μm column (analytical
173 precision of $\pm 1\%$). Cations (Ca, Mg, Na, K, Si) were measured using a SPECTRO Analytical
174 Instruments SPECTROBLUE ICP-OES system (analytical precision of $\pm 2\%$). Trace elements (B,
175 Fe, Mn, Sr) were measured using a Thermo Scientific iCAP TQe ICP-MS system (analytical
176 precision of $\pm 2\%$). Charge balances for all samples were within 5%.

177 ^3H and $\delta^{13}\text{C}$ -DIC analyses were performed at UARizona's Department of Geosciences
178 Environmental Isotopes Laboratory. ^3H was analyzed using a Quantulus 1220 Spectrometer in an
179 underground counting laboratory using electrolytic enrichment and liquid scintillation decay

180 counting methods (Theodorsson 1996), with a detection limit of 0.5 TU. $\delta^{13}\text{C}$ -DIC was analyzed
181 using a ThermoQuest Finnigan Delta PlusXL coupled with a Gasbench automated sampler with a
182 precision of $\pm 0.30\%$ (VPDB).

183 $\delta^{18}\text{O}$ and $\delta^2\text{H}$ were analyzed at the USask's Hillslope Hydrology Lab using a Los Gatos
184 Research liquid water Off-Axis Integrated-Cavity Output Spectrometer. Stable water isotope
185 values are reported in parts per thousand (‰) relative to the Vienna Standard Mean Ocean Water
186 and Standard Light Antarctic Precipitation (VSMOW-SLAP) standards. The 2-sigma uncertainties
187 were ^{18}O (0.8‰) and $\delta^2\text{H}$ (2‰). ^{14}C analyses were performed at the University of Ottawa's Andre
188 E. Lalonde AMS Laboratory on an Ionplus AG MICADAS (Mini Carbon Dating System).
189 Uncertainty on ^{14}C results (1σ) ranged from 0.01–0.07 percent modern carbon (pmC).

190 Noble gases (^4He , $^3\text{He}/^4\text{He}$, Ne, Ar, Kr, Xe) were measured at the University of Utah's
191 Noble Gas Lab. Measurement of all noble gases except helium were completed using a Stanford
192 Research SRS – Model RGA 300 quadruple mass spectrometer; helium was analyzed using a Mass
193 Analyzers Products – Model 215-50 magnetic sector mass spectrometer. Analytical precision for
194 total concentration of the gases was ^3He ($\pm 1\%$), ^4He ($\pm 1\%$), Ne ($\pm 2\%$), Ar ($\pm 2\%$), Kr ($\pm 4\%$) and
195 Xe ($\pm 4\%$).

196 **Radiocarbon Corrections**

197 Uncorrected ^{14}C ages were corrected to account for geochemical reactions occurring in the
198 subsurface—e.g., carbonate mineral dissolution—that impact ^{14}C activity by the addition of “dead
199 carbon” (0 pmC ^{14}C), artificially increasing the apparent groundwater age (Clark and Fritz 1997).
200 To make these corrections, NetpathXL (Parkhurst and Charlton 2008), a revised version of
201 NETPATH (Plummer et al. 1994), was used. NetpathXL employs the revised Fontes and Garnier
202 model (Han and Plummer 2013) and performs basic inverse modeling, based upon the major ion

203 chemistry, $\delta^{13}\text{C}$ -DIC, and radiocarbon values. The program then plots sample points on a graph,
 204 which depending on where the samples plot, indicates whether the Tamers model, gas exchange
 205 model, or solid exchange model should be used in radiocarbon age corrections. In this study, the
 206 ^{14}C was assumed to be 100 pmC, and the ^{14}C and $\delta^{13}\text{C}$ of carbonate minerals were assumed to be
 207 0 pmC and 0‰, respectively. The $\delta^{13}\text{C}$ of soil CO_2 was assumed to be -25‰, which is within the
 208 range of -22.9‰ to -26.8‰ found in soils in Saskatchewan (Landi et al. 2003).

209 Helium-4 Corrections

210 The contributions from atmospheric, mantle, and crustal sources to ^4He were deconvolved
 211 to assist with interpretation of ^4He concentrations. Crustal sources ($^4\text{He}_{\text{rad}}$), which accumulate in
 212 groundwater over time, are of primary interest in assessing groundwater ages in this study.
 213 Atmospheric ^4He contributions can be determined using the $^4\text{He}/^{20}\text{Ne}$ ratio, given that ^4He and
 214 ^{20}Ne have similar solubilities and assuming that ^{20}Ne is solely atmospheric using the following
 215 equation (Hilton 1996):

$$216 \quad R_C = \frac{R_S X - R_A}{X - 1} \quad [1]$$

217 where $X = \left(\frac{^4\text{He}}{^{20}\text{Ne}} \right)_S / \left(\frac{^4\text{He}}{^{20}\text{Ne}} \right)_A$, R is the $^3\text{He}/^4\text{He}$ ratio, and the subscripts C , S , and A stand for the
 218 air-corrected, sample (i.e., measured), and air values, respectively. The $^4\text{He}/^{20}\text{Ne}$ of air ≈ 0.319 ;
 219 values close to this indicate greater atmospheric ^4He inputs, while samples with higher crustal ^4He
 220 inputs typically have a $^4\text{He}/^{20}\text{Ne}$ orders of magnitude higher than air (Ballentine et al. 1996). From
 221 here, the air-corrected $^3\text{He}/^4\text{He}$ ratio (R_C) can be used in an endmember mixing model to determine
 222 the mantle and crustal contributions, using the equation below:

$$223 \quad R_C = f_m R_m + f_{\text{rad}} R_{\text{rad}} \quad [2]$$

224 where subscripts m and rad represent the mantle and radiogenic crustal components, f is
 225 the fractional contribution to the measured sample from the mantle or crust, and R is $^3\text{He}/^4\text{He}$ ratio.
 226 Values in the literature suggest R_m ranges from 8–30 R_A (where R_A is the measured ratio in air;
 227 Saar et al. 2005), while R_{rad} ranges from 0.02–0.05 R_A (Castro et al. 2000). For the purposes of this
 228 research, and in line with past research, $R_m = 8$ and $R_{rad} = 0.02$. The in-situ production can be
 229 determined by removing contributions from air-saturated water ($^4\text{He}_{ASW}$) and the mantle ($^4\text{He}_{mantle}$)
 230 from the measured ^4He ($^4\text{He}_{total}$).

231

$$232 \quad [^4\text{He}_{rad}] = [^4\text{He}_{total}] - [^4\text{He}_{ASW}] - [^4\text{He}_{mantle}] \quad [3]$$

233 $^4\text{He}_{rad}$ can be used to estimate a groundwater age if *in situ* generation and diffusive fluxes into the
 234 aquifer can be estimated. Diffusive fluxes are variable and difficult to characterize in the study
 235 area because transport has not yet reached steady-state due to the relatively young ages of the
 236 sediments present (Hendry et al. 2005; Hendry and Wassenaar 2011). Due to this limitation, we
 237 use $^4\text{He}_{rad}$ concentrations to support interpretations of other tracers rather than estimating
 238 groundwater ages.

239 RESULTS

240 Field Parameters, Major Ions, Trace Elements

241 Field parameters (Table 1), alkalinity, and major ions of groundwater samples were
 242 measured at all 12 observation wells (Table 2). Temperature ranged from 5.9–10.6 °C, pH ranged
 243 from 7.10–8.42, and conductivity ranged from 1,300–4,389 $\mu\text{S}/\text{cm}$. Alkalinity ranged from 298–
 244 827 mg/L. Given that all samples had a $\text{pH} < 9$, bicarbonate (HCO_3) was assumed to be the
 245 dominant constituent of alkalinity. In general, four predominant groundwater types were observed:
 246 Ca-Mg-SO₄ (Saskatoon, Dalmeny, Tessier, Conquest 500, Conquest 502), Na-SO₄ (Tyner,

247 Vanscoy, Nokomis), Ca-Mg-HCO₃ (Agrium, Unity, Lilac), and Na-HCO₃ (Hearts Hill) (Figure 3).
248 Finally, nitrate (NO₃) was detected at the intertill wells at Dalmeny and Conquest 500, with
249 concentrations ranging from 0.12–15.0 mg/L. Vanscoy was the only buried valley well with
250 detectable NO₃, with a concentration of 1.14 mg/L. The bedrock well at Heart's Hill had a NO₃
251 concentration of 6.9 mg/L.
252

253 **Table 1:** Well Details Including Location, Screening, Hydraulic Head, & Field Parameters

Well	Stratigraphic Unit	Aquifer Type	Date Sampled	Latitude	Longitude	Surface Elevation (masl)	Top of Screened Interval (masl)	Bottom of Screened Interval (masl)	Hydraulic Head (masl)
Agrium	Floral	Intertill	06/11/2022	52.026	-107.1	499.9	484.9	482.2	496.9
Conquest 500	Floral Formation	Intertill	06/13/22	51.574	-107.174	554.8	537.6	536	542.9
Dalmeny	Floral	Intertill	06/11/2022	52.261	-106.719	515.1	491.6	490.4	506.9
Saskatoon	Floral	Intertill	06/10/2022	52.172	-106.532	510.5	484.6	483.4	499.4
Tessier	Floral	Intertill	06/12/2022	51.881	-107.514	554.7	530	528.8	545
Unity	Intertill (unclassified)	Intertill	06/16/22	52.465	-108.955	672.1	646.5	645.3	657
Conquest 502	Saskatoon Group	Intertill	06/13/22	51.57	-107.314	571.6	554	552.8	562.1
Lilac	Empress	Buried Valley	06/15/22	52.758	-107.917	548.6	427.3	426.1	538.7
Nokomis	Empress	Buried Valley	06/17/22	51.505	-105.067	509.9	413	410	508.9
Tyner	Empress	Buried Valley	06/12/2022	51.024	-108.424	592.8	480.7	479.1	583.2
Vanscoy	Empress	Buried Valley	06/15/22	52.007	-107.049	512.1	426.7	423.4	507

THIS VERSION HAS BEEN PEER-REVIEWED BUT NOT YET ACCEPTED

Hearts Judith River Bedrock 06/16/22 52.084 -109.564 688.8 613.5 612 680.8

Hill

254 Notes: All wells have a single screened interval; this section is the bottom/end of well construction. Hydraulic heads measured prior

255 to purging.

256

257 **Table 2:** Field parameters and concentrations of anions, cations, and select trace elements for
 258 well samples. Units in mg/L for all analytes. F and Br are not included in table as they were below
 259 the method detection limit in all samples.

260

Well	pH	Temp	EC	Ca	Mg	Na	K	Si	B	Fe	Mn	Sr	Cl	HCO ₃	SO ₄	NO ₃
Agrium	7.41	7.6	145	111	36.9	106	7.79	10.4	0.58	2.69	0.19	0.77	19.6	595	207	<0.8
			9													
Conquest 500	7.71	9.2	360	528	186	40.1	15.9	9.47	0.07	10.6	4.79	1.45	0.94	298	2000	15
			4													
Dalmeny	7.32	6.5	327	367	181	95.4	11.8	10.9	0.56	10.8	0.28	2.31	6.59	827	1300	13.9
			2													
Saskatoon	7.10	8.8	438	419	283	199	17.4	9.40	0.84	16.9	0.34	3.09	44.3	568	2240	<0.8
			9													
Tessier	7.23	10.4	173	145	83.9	77.3	6.15	9.05	0.23	1.96	1.09	0.77	8.7	449	533	<0.8
			5													
Unity	7.16	6.6	130	128	64	26.4	9.19	8.46	0.09	1.54	0.50	0.66	7.2	561	234	<0.8
			0													
Conquest 502	7.25	10.6	187	193	78.3	71.8	10.2	11.7	0.43	1.77	1.36	1.08	20.2	417	622	<0.8
			5													
Lilac	7.94	6.8	161	83.9	60	109	10.7	10.8	0.31	0.77	0.09	0.60	21.7	582	254	<0.8
			8													
Nokomis	7.46	7.0	425	167	83.4	570	8.72	11.8	0.61	2.96	0.14	1.52	283	471	1270	<0.8
			2													
Tyner	8.18	6.9	394	68.6	89.8	612	9.09	5.95	0.85	0.49	0.02	1.23	121	700	1210	<0.8
			1													
Vanscoy	8.42	6.7	375	30.4	27.7	681	5.44	11.2	1.17	0.31	0.02	0.55	256	568	892	1.14
			9													

Heart's 7.96 5.9 150 16.1 14.5 258 8.93 8.97 0.55 0.25 0.05 0.58 5.7 635 210 6.79
 Hill 6

261 **Stable Isotopes**

262 Stable water isotope values ranged from -21.1 to -16.2‰ and -163 to -137‰ for δ¹⁸O and
 263 δ²H, respectively (Table 3; Figure 4). Most samples plot on or below the Local Meteoric Water
 264 Line (LMWL) for Saskatoon (Koehler 2019), given by δ²H =
 265 (δ¹⁸O × 7.69 ± 0.096) – 2.22 ± 1.72. The LMWL for Saskatoon has a lower slope and different
 266 y-intercept than the GMWL (Craig 1961), where δ²H = (δ¹⁸O × 8.0) + 10, consistent with
 267 Saskatoon’s semi-arid climate. Given the strong correlation between δ¹⁸O and δ²H values of
 268 groundwater samples ($R^2 = 0.967$; $P = 4.33 \times 10^{-15}$), further discussion of stable water isotopes will
 269 be limited to δ¹⁸O.

270 **Table 3:** Stable & Radioactive Isotopes. ^aTrace detection below method detection limit. For
 271 laboratory uncertainties, refer to the Methods section.

272

Well	δ ¹⁸		³ H	δ ¹³ C - ¹⁴ C		¹⁴ C (corrected)	
	O	δ ² H		DIC	¹⁴ C (raw)		¹⁴ C (uncorrected)
	‰	‰	TU	‰	pmC	ka	
Agrium	-21.1	-163	ND/< 0.5	-12.6	16.1	14.7	10.1
Conquest	-19.7	-156	2.9	-11.9	34.3	8.6	3.5
500							
Dalmeny	-19.1	-147	0.9	-12.2	15.9	14.5	10.3
Saskatoon	-19.6	-153	0.7	-13.0	8.8	19.5	15.5
Tessier	-19.3	-150	< 0.6 ^a	-12.4	33.5	8.8	4.3
Unity	-16.2	-134	ND/< 0.5	-12.2	62.0	3.8	0

Conquest	-20.6	-160	ND/< 0.5	-12.0	21.2	12.5	8.0
502							
Lilac	-16.9	-137	ND/< 0.5	-12.3	28.0	12.2	5.0
Nokomis	-18.5	-146	ND/< 0.5	-16.8	0.69	40.0	43.1
Tyner	-20.6	-162	ND/< 0.5	-18.8	< 0.51	> 42.5	> 42.5
Vanscoy	-19.5	-154	ND/< 0.5	-18.8	< 0.51	> 42.5	> 42.5
Hearts Hill	-18.4	-149	ND/< 0.5	-12.8	14.9	15.2	10.2

273 **Radioactive Isotope Age Tracers**

274 ^3H was detected at four locations: Saskatoon (0.7 ± 0.28 TU), Dalmeny (0.9 ± 0.31 TU),
 275 Conquest 500 (2.9 ± 0.18), and Tessier (< 0.6 TU; apparent 0.3 ± 0.21 TU) (Table 3). In the other
 276 remaining wells, ^3H was below the detection limit. ^{14}C was detected at ten of twelve locations with
 277 uncorrected ^{14}C ranging from 0.69–62.0 pmC. At Tyner and Vanscoy, ^{14}C was non-detect (< 0.51
 278 pmC). Geochemical modeling using NetPathXL (Parkhurst and Charlton 2008) produced
 279 corrected ^{14}C ‘ages’ ranging from modern to 43.1 ka; excluding Nokomis (43.1 ka), groundwater
 280 ^{14}C ages were much younger, ranging from modern to 15.5 ka (Figure 5). ^{14}C ages were insensitive
 281 to the $\delta^{13}\text{C}$ value used with the exception of the use of low $\delta^{13}\text{C}$ values for the Nokomis sample,
 282 which would result in an ^{14}C age of 49.5 ka.

283 **Noble Gases**

284 Noble gas (He, Ne, Ar, Kr, Xe) concentrations were measured at all twelve locations,
 285 however the focus of this study pertains to the light noble gases (He, Ne, Ar) and their pertinent
 286 isotope relationships ($^3\text{He}/^4\text{He}$, $^4\text{Ne}/^{20}\text{Ne}$, $^{40}\text{Ar}/^{36}\text{Ar}$) (Table 4). Air corrected R_c/R_a values ranged
 287 from 0.008–0.332, with estimated mantle contributions of ^4He ranging from 0.0–3.9% (Table 4).
 288 $^4\text{He}_{\text{rad}}$ varied from 0.37×10^{-7} to 26.2×10^{-7} cm^3 STP/g in intertill aquifers. Samples from buried
 289 valley aquifers had higher concentrations (171 to 331×10^{-7} cm^3 STP/g), except for Lilac ($13 \times$

290 10^{-7} cm³ STP/g). This pattern of ⁴He_{rad} concentrations is consistent with an expected increase
291 associated with greater residence times. The ⁴⁰Ar/³⁶Ar in all samples are in excess of that expected
292 in air-saturated water (366-819 vs 298.56): these excesses do not correlate with radiocarbon and
293 are likely due to interactions with other fluids in the system. Noble gas recharge temperatures are
294 not given for the aquifer due to their probabilities below the acceptable minimum (Jeung et al
295 2018).

296

297 **Table 4:** He, Ne, Ar Concentrations & Isotopic Ratios. ^aAir-corrected. ^bCorrection not applied,
 298 results indicative of field or laboratory fractionation of noble gases. Concentrations for He and
 299 Ne are cm³ STP/g. See methods section for analytical error associated with noble gases. R_c = air-
 300 corrected, f_{rad} = estimated fraction of crustal-derived ⁴He, f_m = estimated fraction of mantle-
 301 derived ⁴He.

302

Well	³ He x 10 ⁻¹³ cm ³ STP/g	⁴ He x 10 ^{-7a} cm ³ STP/g	R _c /R _a	²⁰ Ne x 10 ⁻⁷ cm ³ STP/g	²² Ne x 10 ⁻⁸ cm ³ STP/g	³⁶ Ar x 10 ⁻⁷ cm ³ STP/g	⁴⁰ Ar x 10 ⁻⁴ cm ³ STP/g	f _{rad}	f _m	⁴ He _{rad} 10 ⁻⁷ cm ³ STP/g
Agrium	10.9	26.41	0.274	2.17	2.05	13.4	4.90	0.968	0.032	25.57
Conquest	0.092	0.065		0.21	0.20	0.32	0.22			
500 ^b			1.025					c	c	c
Dalmeny	2.8	4.538	0.220	3.69	3.57	11.5	6.01	0.975	0.025	4.425
Saskatoon	11.4	27.06	0.275	2.82	2.61	9.24	4.66	0.968	0.032	26.19
Tessier	2.25	3.680	0.251	2.44	2.26	9.05	4.60	0.971	0.029	3.574
Unity	1.22	0.386	0.332	2.61	2.43	11.5	4.55	0.961	0.039	0.371
Conquest	1.73	3.082		2.00	1.90	8.85	4.38			
502			0.219					0.975	0.025	3.005
Lilac	6.07	13.65	0.266	2.61	2.45	9.86	4.73	0.969	0.031	13.23
Nokomis	74.7	199.0	0.266	3.48	3.27	9.14	5.35	0.969	0.031	192.9
Tyner	49.0	174.5	0.195	4.94	4.68	12.1	9.91	0.978	0.022	170.7
Vanscoy	133	342.3	0.278	2.77	2.72	12.4	4.80	0.968	0.032	331.2
Hearts Hill	0.96	1.124	0.008	2.38	2.20	9.06	4.54	1.000	0.000	1.126

303

304 DISCUSSION

305 *Interpretation of Sources of Recharge and Groundwater Flow Systems*

306 Groundwater ages extend from modern to over 40,000 years, which includes the final
307 advance of the Laurentide Ice Sheet over the region. The study area is thought to have been free
308 of glacial ice for most of the period between ~75 to 30 ka (Dalton et al. 2022; Dredge and
309 Thorleifson 1987; Wassenaar and Hendry 2000) and after ~12 ka (Christiansen 1979; Dalton et al.
310 2020) (Figure 6). All ^{14}C ages except one correspond to times when the region was ice free,
311 suggesting that, in contrast to some bedrock aquifers in the region (Grasby et al. 2000; Grasby and
312 Chen 2005; Ferguson et al. 2007), the bulk of groundwater present in these systems today did not
313 originate as glacial recharge.

314 Groundwater in the intertill aquifers had corrected ^{14}C ages ranging from 0.0–10.3 ka, aside
315 from one well (Saskatoon) with an age of 15.5 ka and $^4\text{He}_{\text{rad}}$ in these wells are up to 26.19×10^{-7}
316 $\text{cm}^3 \text{ STP/g}$ (Figure 5). These ages are younger than the youngest glacial tills in the study area
317 (Christiansen 1979, 1992), indicating that recharge has been occurring throughout the Holocene.
318 Pleistocene waters are retained in tills in some locations in Saskatchewan (Wassenaar and Hendry
319 2000) but the ages measured here indicate that these tills do not prevent recharge to the underlying
320 intertill aquifers at regional scales. The presence of ^3H at Saskatoon, Dalmeny, Conquest and
321 Tessier, which was sourced from nuclear weapons testing in the 1960s (Clark and Fritz 1997;
322 Gleeson et al. 2016; Lindsey et al. 2019), indicates that modern recharge is present in some areas.
323 NO_3 , which commonly indicates that groundwater has been affected by fertilizer and/or manure
324 application in agricultural areas (Burow et al. 2010; Power and Schepers 1989; Wick et al. 2012),
325 is present at elevated concentrations of 6.79, 13.9, 15.0 mg/L at Heart's Hill, Dalmeny and
326 Conquest 500 respectively, which is also indicative of the presence of modern recharge. The
327 measured NO_3 at Vanscoy (1.1 mg/L) likely has an anthropogenic source. Past sampling of this
328 well has found NO_3 concentrations as high as 15.5 mg/L in 1977 followed by non-detects in the

329 1980s and another increase to 9.2 mg/L in 2004 (Saskatchewan Water Security Agency 2024a).
330 Such variations could be the result of recharge through leaky wells. Mixing of modern waters at
331 other locations could also be the result of leaky wells (Jasechko et al. 2017), diffusion of older
332 groundwater from adjacent aquitards (Bethke and Johnson 2002) or contributions of young and
333 old groundwaters by the different flowpaths intersected along a well screen (Jurgens et al. 2012).

334 The major ion chemistry is consistent with the expected geochemical evolution of
335 groundwater with age (Palmer and Cherry 1984). Intertill aquifers contain Ca-Mg-HCO₃ and Ca-
336 Mg-SO₄ waters (Figure 3), which are typical for younger waters. Na-HCO₃-SO₄ waters are found
337 in buried valley samples except Lilac, where Ca-Mg-HCO₃ water is found along with much
338 younger ages than other buried valley samples. The bedrock sample from Heart's Hill contains
339 Na-HCO₃ water, which is consistent with other lower salinity samples from the Judith River
340 Formation in Saskatchewan (Ferris et al. 2017; McMonagle 1987). Piper plots using larger datasets
341 from the region show considerable variability in the major ion composition of groundwater found
342 in both intertill and buried valley aquifers (MDH Engineered Solutions Ltd. 2011; McMonagle
343 1987). Whether this variability can be related to groundwater age for these larger datasets, where
344 age tracers were not measured or reported, is unclear.

345 Groundwater ages closer to the LGM are present at the Saskatoon well, and have also been
346 observed in Sutherland Group tills in the study area, where uncorrected ¹⁴C ages ranging from
347 19.9–24.8 ka were observed (Keller et al. 1988). The range of ages in this study indicates there has
348 been active subregional groundwater flow systems in these aquifers since they became confined
349 during the deposition of Late Wisconsinan tills. For example, the Dalmeny aquifer has a modern
350 hydraulic gradient of ~0.001 to 0.002 over a flow system ~ 10 km in length (Fortin et al. 1991).
351 The aquifer has a typical porosity of 0.30 and hydraulic conductivity of 10⁻⁶ to 10⁻³ m/s (MDH

352 Engineered Solutions Ltd. 2011; Meneley et al. 1979). This gradient, hydraulic conductivity, and
353 porosity provide a groundwater velocity of ~0.1 to 200 m/yr. These velocities result in aquifer
354 transit times that are of 50 to 100,000 years. This 10.3 ka ¹⁴C age found near the Dalmeny aquifer's
355 southeast discharge area suggests that the effective hydraulic conductivity is in the lower part of
356 the range of hydraulic conductivities, assuming a piston flow model. The presence of elevated NO₃
357 suggests that the bulk age is a mixture of older groundwaters and modern recharge and that piston
358 flow may not accurately describe the flow system. The increase in hydraulic gradients toward the
359 discharge zones shown by Fortin et al. (1991) suggest that recharge is occurring through the
360 overlying tills over much of the aquifer. The mixed groundwater ages may reflect the presence of
361 younger water associated with flowpaths intersected in the upper portion of the well screen, while
362 the lower part of the well screen samples older groundwater. This mixing process has been
363 explored in detail by Jurgens et al (2012). This may provide a conceptual model for other intertill
364 aquifers in the study area that have similar ¹⁴C ages along with contributions of modern recharge.

365 Recharge reaching intertill aquifers must pass through overlying tills. A compilation of
366 hydraulic conductivities for tills in Saskatchewan revealed in situ values of 5.5×10^{-9} m/s for
367 measurements at depths of less than 10 m, 1.9×10^{-9} m/s for depths between 10 and 23 m $1.8 \times 10^{-$
368 ¹⁰ m/s at depths greater than 23 m, with the reduction in permeability attributed to the transition
369 between oxidized and unoxidized conditions (Ferris et al. 2020). Values in the upper two depth
370 intervals were much more variable than those in the lower interval due the presence of fractures.
371 Estimates of Darcy velocities in the deeper tills are as low as 10^{-4} m/yr, which is corroborated by
372 diffusion-dominated transport (Hendry and Wassenaar 1999). In the higher hydraulic conductivity
373 oxidized tills, Darcy velocities a few orders of magnitude greater are possible. Hydrostratigraphic
374 cross-sections of the region indicate that oxidized tills directly overlie Floral Formation aquifers

375 in some areas (MDH Engineered Solutions Ltd. 2011). These areas are possible pathways for
376 recharge, especially if they correspond with upland wetlands.

377 The persistence of older water in the Tyner Valley (Tyner and Vanscoy) and Hatfield
378 Valley aquifers (Nokomis) indicates that the aquifers have not been flushed during or since the
379 LGM, perhaps due to presence of older tills during the Late Wisconsinan glaciation. Groundwater
380 age does not have an obvious relationship with what can be inferred about the regional
381 groundwater flow systems in these aquifers from the limited data available. In the Tyner Valley
382 aquifer, the sample from Tyner has a ${}^4\text{He}_{\text{rad}}$ concentration of $170.7 \times 10^{-7} \text{ cm}^3 \text{ STP/g}$ and the
383 sample from Vanscoy, which is ~150 km to the northeast, has a concentration of $331.2 \times 10^{-7} \text{ cm}^3$
384 STP/g. At Nokomis, a ${}^4\text{He}_{\text{rad}}$ value of $192.9 \times 10^{-7} \text{ cm}^3 \text{ STP/g}$ was measured, suggesting that the
385 age of the groundwater at Tyner is just beyond the limit of ${}^{14}\text{C}$ dating and that ages at Vanscoy
386 could be considerably older. Hydraulic head is ~582 masl at Tyner and ~508 masl at Vanscoy
387 which could indicate that the higher ${}^4\text{He}$ concentrations are present in the downgradient location.
388 However, the dearth of hydraulic head and tracer measurements create some uncertainty around
389 this interpretation. Groundwater flow at Tyner could be southwards towards the South
390 Saskatchewan River (Meneley et al. 1979), which has a hydraulic head value of ~554 masl at that
391 location. However, responses of this aquifer to pumping nearby suggest the presence of low
392 permeability barriers that may prevent regional flow (Maathuis 2005). Groundwater flow at
393 Vanscoy is thought to be northward (Meneley et al. 1979) but the discharge area is unclear. The
394 South Saskatchewan River has an elevation of ~470 masl at Saskatoon while a well Warman has
395 a hydraulic head value of 452 masl, suggesting downward flow from the South Saskatchewan
396 River towards the Tyner Valley aquifer. There is little pumping in this area (Saskatchewan Water
397 Security Agency 2024b), suggesting that gradients are the result of background conditions.

398 Discharge appears to occur further to the northeast downstream of the confluence of the North and
399 South Saskatchewan rivers. Little is known about the flow system within Hatfield Valley aquifer
400 at Nokomis. Discharge from this system may be occurring into Last Mountain Lake to the east
401 (Meneley et al. 1979) or to the Qu'Appelle River Valley to the south.

402 The one bedrock aquifer sample taken in this study was from the Judith River Formation
403 and had a corrected ^{14}C age of 10.2 ka and a NO_3 concentration of 6.79 mg/L, indicating a
404 component of modern recharge. Flow in this region was previously thought to be to the northeast
405 (Meneley et al. 1979) but more recent mapping of the potentiometric surface in this region
406 indicates that groundwater flow is towards the south in this region with discharge occurring to the
407 South Saskatchewan River approximately 20 km south of the well that was sampled (Ferris et al.
408 2017). Till covers much of the region surrounding this well and recharge likely occurs in areas
409 where aquitards are thinner due to nondeposition or erosion but this region has yet to be mapped
410 in detail.

411 *Use of $\delta^2\text{H}$ and $\delta^{18}\text{O}$ as Groundwater Tracers in Saskatchewan*

412 Multiple studies of groundwater in bedrock aquifers in the Canadian Prairies have used a
413 shift in $\delta^2\text{H}$ and $\delta^{18}\text{O}$ values similar to those in modern recharge to lower values as an indication
414 of the presence of Pleistocene meltwater (Ferguson et al. 2007; Grasby et al. 2000; Grasby and
415 Chen 2005) but such a shift is not obvious in the data collected in this study (Figure 7). In intertill
416 aquifer samples, $\delta^{18}\text{O}$ values range from -21.1 to -16.2‰. In samples with ^{14}C ages < 5 ka, $\delta^{18}\text{O}$
417 values are between -19.7 and -16.2‰, while the Saskatoon sample, with ^{14}C age of 15.5 ka has a
418 $\delta^{18}\text{O}$ value of -19.6‰. $\delta^{18}\text{O}$ values associated with older groundwater samples in buried valley
419 aquifers have values of -20.6 to -18.5‰. Aside from the samples with the highest $\delta^{18}\text{O}$ values at

420 Lilac and Unity, which appear to be affected by evaporation, there is considerable overlap in the
421 $\delta^{18}\text{O}$ values from samples with ages corresponding to the Pleistocene and Holocene.

422 Values of approximately -21 to -18‰ have been interpreted as Pleistocene in age within
423 glacial tills based on groundwater ages and transport modelling (Hendry et al. 2004; Keller et al.
424 1988) but this also overlaps with modern precipitation in the Saskatoon region (Koehler 2019), as
425 well as shallow groundwater (Clark and Fritz 1997; Keller et al. 1988; Hendry et al. 2004; Hendry
426 and Wassenaar 1999; Bam et al. 2020; McMonagle 1987). Groundwater $\delta^2\text{H}$ and $\delta^{18}\text{O}$ in the
427 region, including previous analyses of intertill aquifers and buried valley wells sampled in this
428 study, have been explained by recharge from modern precipitation without a need to consider a
429 paleo-recharge component (McMonagle 1987).

430 Seasonal changes in hydraulic head have been invoked as evidence of the timing of
431 recharge to both intertill and buried valley aquifers (McMonagle 1987). Subsequent research in
432 Saskatchewan, including some of the wells sampled by McMonagle (1987), has shown that these
433 variations in hydraulic head are the result of downward hydraulic diffusion of changes in total
434 stress from soil moisture loading rather than recharge reaching confined aquifers (van der Kamp
435 and Maathuis 1991; Anochikwa et al. 2012; van der Kamp and Schmidt 1997). This is corroborated
436 by corrected ^{14}C ages from the current study indicating that a considerable fraction of groundwater
437 at these locations is not modern recharge. This suggests that either the climate and recharge
438 mechanisms have been relatively stable throughout the Holocene and late Pleistocene or that
439 different climates and recharge mechanisms have resulted in similar $\delta^2\text{H}$ and $\delta^{18}\text{O}$ values.

440 Conditions during the early Holocene were more arid than those currently observed (Wolfe
441 et al. 2002), which would have also emphasized winter precipitation in recharge. Increased aridity
442 conditions may explain the presence of $\delta^2\text{H}$ and $\delta^{18}\text{O}$ values that plots beneath the GMWL

443 associated with an early Holocene corrected ^{14}C date at the Lilac well. $\delta^2\text{H}$ and $\delta^{18}\text{O}$ values at the
444 Saskatoon well, which has a corrected ^{14}C date that coincides with a time when the region was
445 glaciated, is similar to modern winter precipitation in the Saskatoon region. The climate conditions
446 associated with the much older groundwater ages at Vanscoy, Nokomis and Tyner have not been
447 characterized in detail. The similarity with other $\delta^2\text{H}$ and $\delta^{18}\text{O}$ values could indicate similar climate
448 conditions. Coincidence of $\delta^2\text{H}$ and $\delta^{18}\text{O}$ values in groundwater with modern precipitation is not
449 an indicator that modern recharge is present. $\delta^2\text{H}$ and $\delta^{18}\text{O}$ values are similar for groundwater with
450 a wide range of groundwater ages, making these measurements less useful in the study area than
451 they are in other regions.

452 *Implications for Groundwater Management*

453 The geochemical and isotopic measurements made in this study indicate that a range of
454 groundwater ages, from fossil to modern, exist in intertill and buried valley aquifers in the
455 Saskatoon region. Modern recharge and much older groundwater are often present the same wells,
456 underscoring the need to use multiple tracers that provide information over different age ranges.
457 Recharge to confined intertill aquifers is occurring despite the widespread presence of low
458 hydraulic conductivity tills and lack of obvious recharge areas. This underscores a need for
459 groundwater protection measures in Saskatchewan and more generally.

460 The presence of a continuum of groundwater ages including modern recharge indicates that
461 groundwater resources in the region could be renewable if developed at a suitably low level.
462 Groundwater age is a function of both recharge rate and distance from the point of recharge along
463 a flowpath (Ferguson et al. 2020). The sparsity of the observation well network and lack of other
464 reliable hydraulic head measurements make it difficult to determine the position of observation
465 wells relative to recharge areas. As a result, groundwater recharge rates cannot reliably be

466 determined with the groundwater ages estimated in this study. Additionally, recharge rates
467 themselves are insufficient to assess whether groundwater is renewable because they are not
468 critical to predicting hydraulic responses of groundwater to pumping (Cuthbert et al. 2023;
469 Konikow and Leake 2014). However, the presence of modern recharge is generally considered to
470 be a minimum requirement to allow for development of groundwater resources, particularly where
471 older groundwaters are present (Margat et al. 2006; Bierkens and Wada 2019).

472 Understanding what level of development is possible will require more detailed hydraulic
473 characterization of aquifers in the region to understand the potential impacts of pumping to
474 hydraulic heads in existing and future wells and groundwater-surface water interactions.

475 Single well tests were conducted at most SWSA observation wells in the region (Meneley
476 et al. 1979) but these tests may not be sufficient to capture the spatial variability of hydraulic
477 conductivity due the limited number of wells. Published data for these aquifers is also relatively
478 limited (MDH Engineered Solutions Ltd. 2011). An additional challenge is that single wells tests
479 do not provide estimates of storage coefficients (Cooper et al. 1967; Halford et al. 2006), which
480 are necessary to predict the spatial and temporal distribution of drawdown resulting from pumping.
481 Additional multiwell testing in an expanded observation network would improve our
482 understanding of these aquifers. Expansion of the observation well network would also provide
483 opportunities to improve the spatial coverage of hydraulic head and tracer measurements for use
484 in calibrating numerical models that could be used to predict changes in hydraulic head associated
485 with pumping.

486 **SUMMARY & CONCLUSIONS**

487 This study used groundwater age tracers of varying timescales (^3H , ^{14}C , ^4He), stable water
488 isotopes and major ions to examine the recharge history of intertill and buried valley aquifers in

489 southern Saskatchewan, Canada. The majority of groundwater present throughout Saskatoon
490 group intertill aquifers was recharged after the LGM (i.e., < 10.3 ka), and in several areas contains
491 a component of modern recharge (< 60 years old). Pleistocene glacial water, still retained in
492 adjacent till aquitards in the region (Hendry and Wassenaar 1999; Keller et al. 1988), must have
493 been flushed or mixed with younger water by regional groundwater flow in intertill aquifers.
494 Regional flow appears to have been operating in shallow intertill aquifers throughout the Holocene
495 based on the range of radiocarbon ages present in these aquifers. This suggests that groundwater
496 in these aquifers is being replenished under current conditions, although at low rates. Groundwater
497 in the buried valley aquifers of the Empress Group is substantially older than the overlying
498 Saskatoon groups, with recharge likely occurring during interglacial periods from 75–40 ka when
499 southern Saskatchewan was ice-free. Groundwater in the underlying Judith River Bedrock is
500 similar in age to the Saskatoon Group, suggesting a similar recharge mechanism.

501 No trends were observed in $\delta^{18}\text{O}$ and $\delta^2\text{H}$ values compared to groundwater age. This could
502 indicate that recharge mechanisms similar to those observed today have been occurring over
503 millennial timescales but may also reflect different sources of recharge with similar $\delta^{18}\text{O}$ and $\delta^2\text{H}$
504 values. ^3H and NO_3 provided clearer evidence that a component of modern groundwater is being
505 recharged to these aquifers. ^4He measurements were not straightforward to interpret due to issues
506 related to diffusion profiles that have not had time to reach steady state in the Pleistocene sediments
507 of the region, along with noble gas contributions from other fluids. The presence of groundwater
508 with ages measured in millennia and modern groundwater at the same wells underscore the
509 importance of using multiple tracers to characterize groundwater age distributions.

510 **Acknowledgments**

511 Funding for this research was provided by the Geological Survey of Canada. We thank
512 Erin Schmeling from the University of Saskatchewan for providing field equipment for sampling.
513 We would also like to acknowledge Kei Lo and Anatoly Melnik from the Saskatchewan Water
514 Security Agency who provided background information and logistical support in accessing the
515 monitoring well network.

516

517 **References**

- 518 Anochikwa, C. I., G. van der Kamp, and S. L. Barbour. 2012. Interpreting pore-water pressure
519 changes induced by water table fluctuations and mechanical loading due to soil moisture
520 changes. *Canadian Geotechnical Journal* 49, no. 3: 357–66, [https://doi.org/10.1139/t11-](https://doi.org/10.1139/t11-106)
521 106.
- 522 Ballentine, C. J., R. K. O’Nions, and M. L. Coleman. 1996. A Magnus opus: Helium, neon, and
523 argon isotopes in a North Sea oilfield. *Geochimica et Cosmochimica Acta* 60, no. 5: 831–
524 49.
- 525 Bam, E. K., and A. M. Ireson. 2019. Quantifying the wetland water balance: a new isotope-based
526 approach that includes precipitation and infiltration. *Journal of Hydrology* 570: 185–200.
- 527 Bam, E. K., A. M. Ireson, G. van Der Kamp, and J. M. Hendry. 2020. Ephemeral ponds: Are
528 they the dominant source of depression-focused groundwater recharge? *Water Resources*
529 *Research* 56, no. 3: e2019WR026640.
- 530 Bethke, C. M., and T. M. Johnson. 2002. Paradox of groundwater age. *Geology* 30, no. 2: 107–
531 10.
- 532 Bierkens, M. F., and Y. Wada. 2019. Non-renewable groundwater use and groundwater
533 depletion: a review. *Environmental Research Letters* 14, no. 6: 063002.
- 534 Burow, K. R., B. T. Nolan, M. G. Rupert, and N. M. Dubrovsky. 2010. Nitrate in Groundwater
535 of the United States, 1991–2003. *Environmental Science & Technology* 44, no. 13: 4988–
536 97, <https://doi.org/10.1021/es100546y>.
- 537 Case, R. A., and G. M. MacDonald. 2003. Tree Ring Reconstructions of Streamflow for Three
538 Canadian Prairie Rivers. *JAWRA Journal of the American Water Resources Association*
539 39, no. 3: 703–16, <https://doi.org/10.1111/j.1752-1688.2003.tb03686.x>.

- 540 Castro, M. C., M. Stute, and P. Schlosser. 2000. Comparison of 4He ages and 14C ages in simple
541 aquifer systems: implications for groundwater flow and chronologies. *Applied*
542 *Geochemistry* 15, no. 8: 1137–67.
- 543 Christiansen, E. A. 1979. The Wisconsinan deglaciation, of southern Saskatchewan and adjacent
544 areas. *Canadian Journal of Earth Sciences* 16, no. 4: 913–38.
- 545 Christiansen, E. A. 1992. Pleistocene stratigraphy of the Saskatoon area, Saskatchewan, Canada:
546 an update. *Canadian Journal of Earth Sciences* 29, no. 8: 1767–78.
- 547 Clark, I. D., and P. Fritz. 1997. *Environmental isotopes in hydrogeology*. CRC press.
- 548 Cooper, H. H., J. D. Bredehoeft, and I. S. Papadopoulos. 1967. Response of a finite-diameter well
549 to an instantaneous charge of water. *Water Resources Research* 3, no. 1: 263–69.
- 550 Craig, H. 1961. Isotopic variations in meteoric waters. *Science* 133, no. 3465: 1702–3.
- 551 Cummings, D. I., H. A. Russell, and D. R. Sharpe. 2012. Buried-valley aquifers in the Canadian
552 Prairies: geology, hydrogeology, and origin 1 1 Earth Science Sector (ESS) Contribution
553 20120131. *Canadian Journal of Earth Sciences* 49, no. 9: 987–1004.
- 554 Cuthbert, M. O., T. Gleeson, M. F. P. Bierkens, G. Ferguson, and R. G. Taylor. 2023. Defining
555 renewable groundwater use and its relevance to sustainable groundwater management.
556 *Water Resources Research* 59, no. 9: e2022WR032831.
- 557 Dalton, A. S., M. Margold, C. R. Stokes, L. Tarasov, A. S. Dyke, R. S. Adams, S. Allard, H. E.
558 Arends, N. Atkinson, and J. W. Attig. 2020. An updated radiocarbon-based ice margin
559 chronology for the last deglaciation of the North American Ice Sheet Complex.
560 *Quaternary Science Reviews* 234: 106223.

- 561 Dalton, A. S., C. R. Stokes, and C. L. Batchelor. 2022. Evolution of the Laurentide and Inuitian
562 ice sheets prior to the Last Glacial Maximum (115 ka to 25 ka). *Earth-Science Reviews*
563 224: 103875.
- 564 Dawson, F., C. Evans, R. Marsh, and R. Richardson. 1994. Uppermost Cretaceous and Tertiary
565 strata of the Western Canada sedimentary basin. *Geological Atlas of the Western Canada*
566 *Sedimentary Basin, Canadian Society of Petroleum Geologists and Alberta Research*
567 *Council, Calgary*, 18.
- 568 Dredge, L. A., and L. H. Thorleifson. 1987. The Middle Wisconsinan history of the Laurentide
569 ice sheet. *Géographie physique et Quaternaire* 41, no. 2: 215–35.
- 570 Edmunds, W. M. 2003. Renewable and non-renewable groundwater in semi-arid and arid
571 regions. In *Developments in water science*, 50:265–80. Elsevier.
- 572 Environment and Climate Change Canada. 2024. Canadian Climate Normals 1991-2020 Data -
573 Climate, 2024,
574 https://climate.weather.gc.ca/climate_normals/results_1991_2020_e.html?searchType=stnProv&lstProvince=SK&txtCentralLatMin=0&txtCentralLatSec=0&txtCentralLongMin=0&txtCentralLongSec=0&stnID=265000000&dispBack=0.
- 577 Ferguson, G., R. N. Betcher, and S. E. Grasby. 2007. Hydrogeology of the Winnipeg Formation
578 in Manitoba, Canada. *Hydrogeology Journal* 15, no. 3: 573–87,
579 <https://doi.org/10.1007/s10040-006-0130-4>.
- 580 Ferguson, G., M. O. Cuthbert, K. Befus, T. Gleeson, and J. C. McIntosh. 2020. Rethinking
581 groundwater age. *Nature Geoscience* 13, no. 9: 592–94.
- 582 Ferguson, G. and Jasechko, S., 2015. The isotopic composition of the Laurentide Ice Sheet and
583 fossil groundwater. *Geophysical Research Letters* 42, no. 12: 4856-4861.

- 584 Ferris, D. M., M. Lypka, and G. Ferguson. 2017. Hydrogeology of the Judith River Formation in
585 southwestern Saskatchewan, Canada. *Hydrogeology Journal* 25, no. 7: 1985–95,
586 <https://doi.org/10.1007/s10040-017-1611-3>.
- 587 Ferris, D. M., G. Potter, and G. Ferguson. 2020. Characterization of the hydraulic conductivity of
588 glacial till aquitards. *Hydrogeology Journal* 28: 1827–39.
- 589 Fortin, G., G. Van Der Kamp, and J. Cherry. 1991. Hydrogeology and hydrochemistry of an
590 aquifer-aquitard system within glacial deposits, Saskatchewan, Canada. *Journal of*
591 *Hydrology* 126, nos. 3–4: 265–92.
- 592 Gerber, R. E., and K. W. Howard. 1996. Evidence for recent groundwater flow through Late
593 Wisconsinan till near Toronto, Ontario. *Canadian Geotechnical Journal* 33, no. 4: 538–
594 55, <https://doi.org/10.1139/t96-080-302>.
- 595 Gieskes, J. M., and W. C. Rogers. 1973. Alkalinity determination in interstitial waters of marine
596 sediments. *Journal of sedimentary research* 43, no. 1: 272–77.
- 597 Gleeson, T., K. M. Befus, S. Jasechko, E. Luijendijk, and M. B. Cardenas. 2016. The global
598 volume and distribution of modern groundwater. *Nature Geoscience* 9, no. 2: 161–67.
- 599 Grasby, S. E., and R. N. Betcher. 2002. Regional hydrogeochemistry of the carbonate rock
600 aquifer, southern Manitoba. *Canadian Journal of Earth Sciences* 39, no. 7: 1053–63.
- 601 Grasby, S. E., and Z. Chen. 2005. Subglacial recharge into the Western Canada Sedimentary
602 Basin—Impact of Pleistocene glaciation on basin hydrodynamics. *Geological Society of*
603 *America Bulletin* 117, nos. 3–4: 500–514.
- 604 Grasby, S. E., K. Osadetz, R. N. Betcher, and F. Render. 2000. Reversal of the regional-scale
605 flow system of the Williston Basin in response to Pleistocene glaciation. *Geology* 28, no.
606 7: 635–38.

- 607 Halford, K. J., W. D. Weight, and R. P. Schreiber. 2006. Interpretation of transmissivity
608 estimates from single-well pumping aquifer tests. *Groundwater* 44, no. 3: 467–71.
- 609 Han, L.-F., and L. N. Plummer. 2013. Revision of Fontes & Garnier’s model for the initial 14C
610 content of dissolved inorganic carbon used in groundwater dating. *Chemical Geology*
611 351: 105–14.
- 612 Hayashi, M., G. van der Kamp, and D. L. Rudolph. 1998. Water and solute transfer between a
613 prairie wetland and adjacent uplands, 1. Water balance. *Journal of Hydrology* 207, nos.
614 1–2: 42–55.
- 615 Hendry, M. J., S. L. Barbour, K. Novakowski, and L. I. Wassenaar. 2013. Paleohydrogeology of
616 the Cretaceous sediments of the Williston Basin using stable isotopes of water. *Water*
617 *Resources Research* 49, no. 8: 4580–92.
- 618 Hendry, M. J., C. J. Kelln, L. I. Wassenaar, and J. Shaw. 2004. Characterizing the hydrogeology
619 of a complex clay-rich aquitard system using detailed vertical profiles of the stable
620 isotopes of water. *Journal of Hydrology* 293, nos. 1–4: 47–56.
- 621 Hendry, M. J., T. G. Kotzer, and D. K. Solomon. 2005. Sources of radiogenic helium in a clay
622 till aquitard and its use to evaluate the timing of geologic events. *Geochimica et*
623 *Cosmochimica Acta* 69, no. 2: 475–83.
- 624 Hendry, M. J., and L. I. Wassenaar. 1999. Implications of the distribution of δD in pore waters
625 for groundwater flow and the timing of geologic events in a thick aquitard system. *Water*
626 *Resources Research* 35, no. 6: 1751–60.
- 627 Hendry, M. J., and L. I. Wassenaar. 2011. Millennial-scale diffusive migration of solutes in thick
628 clay-rich aquitards: evidence from multiple environmental tracers. *Hydrogeology Journal*
629 19, no. 1: 259.

- 630 Hilton, D. R. 1996. The helium and carbon isotope systematics of a continental geothermal
631 system: results from monitoring studies at Long Valley caldera (California, USA).
632 *Chemical Geology* 127, no. 4: 269–95.
- 633 Jasechko, S., D. Perrone, K. M. Befus, M. B. Cardenas, G. Ferguson, T. Gleeson, E. Luijendijk,
634 J. J. McDonnell, R. G. Taylor, and Y. Wada. 2017. Global aquifers dominated by fossil
635 groundwaters but wells vulnerable to modern contamination. *Nature Geoscience* 10, no.
636 6: 425–29.
- 637 Jurgens, B.C., Böhlke, J.K., and Eberts, S.M., 2012, TracerLPM (Version 1): An Excel®
638 workbook for interpreting groundwater age distributions from environmental tracer data:
639 U.S. Geological Survey Techniques and Methods Report 4-F3, 60 p.
- 640 Kamp, G. van der. 2001. Methods for determining the in situ hydraulic conductivity of shallow
641 aquitards—an overview. *Hydrogeology Journal* 9: 5–16.
- 642 Kamp, G. van der, and H. Maathuis. 1991. Annual fluctuations of groundwater levels as a result
643 of loading by surface moisture. *Journal of Hydrology* 127, nos. 1–4: 137–52.
- 644 Kamp, G. van der, and R. Schmidt. 1997. Monitoring of total soil moisture on a scale of hectares
645 using groundwater piezometers. *Geophysical Research Letters* 24, no. 6: 719–22,
646 <https://doi.org/10.1029/97GL00521>.
- 647 Keller, C. K., G. Van Der Kamp, and J. A. Cherry. 1988. Hydrogeology of two Saskatchewan
648 tills, I. Fractures, bulk permeability, and spatial variability of downward flow. *Journal of*
649 *Hydrology* 101, nos. 1–4: 97–121.
- 650 Koehler, G. 2019. Snow gauge undercatch and its effect on the hydrogen and oxygen stable
651 isotopic composition of precipitation. *Isotopes in Environmental and Health Studies* 55,
652 no. 4: 404–18.

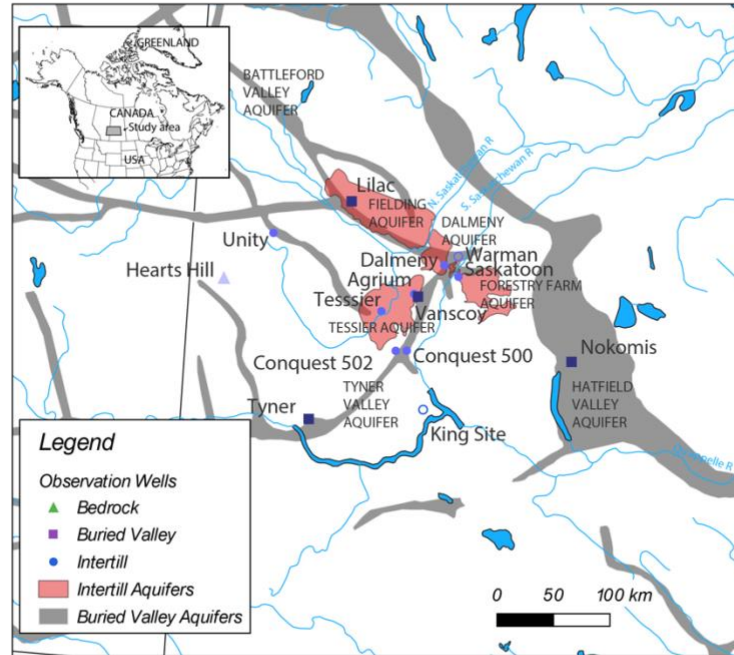
- 653 Konikow, L. F., and S. A. Leake. 2014. Depletion and Capture: Revisiting “The Source of Water
654 Derived from Wells.” *Groundwater* 52, no. S1: 100–111.
- 655 Landi, A., D. W. Anderson, and A. R. Mermut. 2003. Organic carbon storage and stable isotope
656 composition of soils along a grassland to forest environmental gradient in Saskatchewan.
657 *Canadian Journal of Soil Science* 83, no. 4: 405–14, <https://doi.org/10.4141/S02-021>.
- 658 Lemieux, J., E. Sudicky, W. Peltier, and L. Tarasov. 2008. Dynamics of groundwater recharge
659 and seepage over the Canadian landscape during the Wisconsinian glaciation. *Journal of*
660 *Geophysical Research: Earth Surface (2003–2012)* 113, no. F1.
- 661 Lindsey, B.D., Jurgens, B.C., and Belitz, K., 2019, Tritium as an indicator of modern, mixed,
662 and premodern ground-water age: U.S. Geological Survey Scientific Investigations
663 Report 2019–5090, 18 p., <https://doi.org/10.3133/sir20195090>
- 664 Maathuis, H. 2005. Review of Pumping and Recovery Data for the Tyner Valley Aquifer and
665 Impact of Pumping on the Tessier Aquifer. SRC Publication No. 10417-2E05.
- 666 Maathuis, H., B. T. Schreiner, A. Karvonen, J. Fahlman, and N. Shaheen. 2011. Regional
667 geological and groundwater mapping in Saskatchewan: a historical perspective. In
668 *Geohydro 2011 Conference*, 2011. Quebec City, Canada.
- 669 Margat, J., Foster, S. and Droubi, A. 2006. Concept and Importance of Non-Renewable
670 Resources. In: Foster, S. and Loucks, D.P., Eds., *Non-Renewable Groundwater*
671 *Resources: A Guidebook on Socially-Sustainable Management for Water-Policy Makers*,
672 IHP-VI, Series on Groundwater No. 10, UNESCO, Paris, 13-24.
- 673 Martin, F. R. J. 2002. *Gross Evaporation for the 30 Year Period 1971-2000 in the Canadian*
674 *Prairies*. Agriculture and Agri-Food Canada, Prairie Farm Rehabilitation Administration.
675 Hydrology Report 113, 69 p.

- 676 McIntosh, J. C., M. Schlegel, and M. Person. 2012. Glacial impacts on hydrologic processes in
677 sedimentary basins: evidence from natural tracer studies. *Geofluids* 12, no. 1: 7–21.
- 678 McLean, J. R. 1971. Stratigraphy of the Upper Cretaceous Judith River Formation in the
679 Canadian Great Plains. Saskatchewan Research Council Geology Division. Report no.
680 11. 96 p.
- 681 McMonagle, A. L. 1987. Stable isotope and chemical compositions of surface and subsurface
682 waters in Saskatchewan, [https://harvest.usask.ca/items/59516875-0525-491c-943e-](https://harvest.usask.ca/items/59516875-0525-491c-943e-ec73d9f21b03)
683 [ec73d9f21b03](https://harvest.usask.ca/items/59516875-0525-491c-943e-ec73d9f21b03).
- 684 MDH Engineered Solutions Ltd. 2011. Hydrogeology Mapping of NTS Mapsheet Saskatoon
685 73B.
- 686 Meneley, W. A., H. Maathuis, E. J. Jaworski, and V. F. Allan. 1979. *SRC observation wells in*
687 *Saskatchewan, Canada: Introduction, design and discussion of accumulated data*. Vol. 3.
688 19. Saskatoon, Canada: Saskatchewan Research Council.
- 689 Mowat, A. C., D. J. Francis, J. C. McIntosh, M. B. Lindsay, and G. A. Ferguson. 2021.
690 Variability in timing and transport of Pleistocene meltwater recharge to regional aquifers.
691 *Geophysical Research Letters* 48, no. 20: e2021GL094285.
- 692 North Greenland Ice Core Project members. 2004. High-resolution record of northern
693 hemisphere climate extending into the last interglacial period. *Nature* 431: 147–51.
- 694 Palmer, C. D., and J. A. Cherry. 1984. Geochemical evolution of groundwater in sequences of
695 sedimentary rocks. *Journal of Hydrology* 75, nos. 1–4: 27–65.
- 696 Parkhurst, D.L., and Charlton, S.R., 2008, NetpathXL—An Excel® interface to the program
697 NETPATH: U.S. Geological Survey Techniques and Methods 6-A26, 11 p.

- 698 Peel, M. C., B. L. Finlayson, and T. A. McMahon. 2007. Updated world map of the Köppen-
699 Geiger climate classification. *Hydrology and Earth System Sciences* 11, no. 5: 1633–44.
- 700 Person, M., J. McIntosh, V. Bense, and V. Remenda. 2007. Pleistocene hydrology of North
701 America: the role of ice sheets in reorganizing groundwater flow systems. *Reviews of*
702 *Geophysics* 45, no. 3.
- 703 Plummer, L. N., E. C. Prestemon, and D. L. Parkhurst. 1994. An interactive code (NETPATH)
704 for modeling net geochemical reactions along a flow path, version 2.0. *Water-Resources*
705 *Investigations Report* 94: 4169.
- 706 Power, J. F. Y., and J. S. Schepers. 1989. Nitrate contamination of groundwater in North
707 America. *Agriculture, ecosystems & environment* 26, nos. 3–4: 165–87.
- 708 Rodvang, S., and W. Simpkins. 2001. Agricultural contaminants in Quaternary aquitards: A
709 review of occurrence and fate in North America. *Hydrogeology Journal* 9: 44–59.
- 710 Ruff, S. E., P. Humez, I. H. de Angelis, M. Diao, M. Nightingale, S. Cho, L. Connors, O. O.
711 Kuloyo, A. Seltzer, and S. Bowman. 2023. Hydrogen and dark oxygen drive microbial
712 productivity in diverse groundwater ecosystems. *Nature Communications* 14, no. 1: 3194.
- 713 Saskatchewan Water Security Agency. 2024a. Groundwater Observation Well Network, 2024,
714 <https://www.wsask.ca/Water-Info/Ground-Water/Observation-Wells/>.
- 715 Saskatchewan Water Security Agency. 2024b. Water Wells GIS Site, 2024,
716 <https://gis.wsask.ca/Html5Viewer/index.html?viewer=WaterWells.WellsViewer/>.
- 717 Solomon, D. K., and P. G. Cook. 2000. ^3H and ^3He . In *Environmental tracers in subsurface*
718 *hydrology*, 397–424. Springer.
- 719 Theodorsson, P. 1996. *Measurement of weak radioactivity*. River Edge, New Jersey: World
720 scientific.

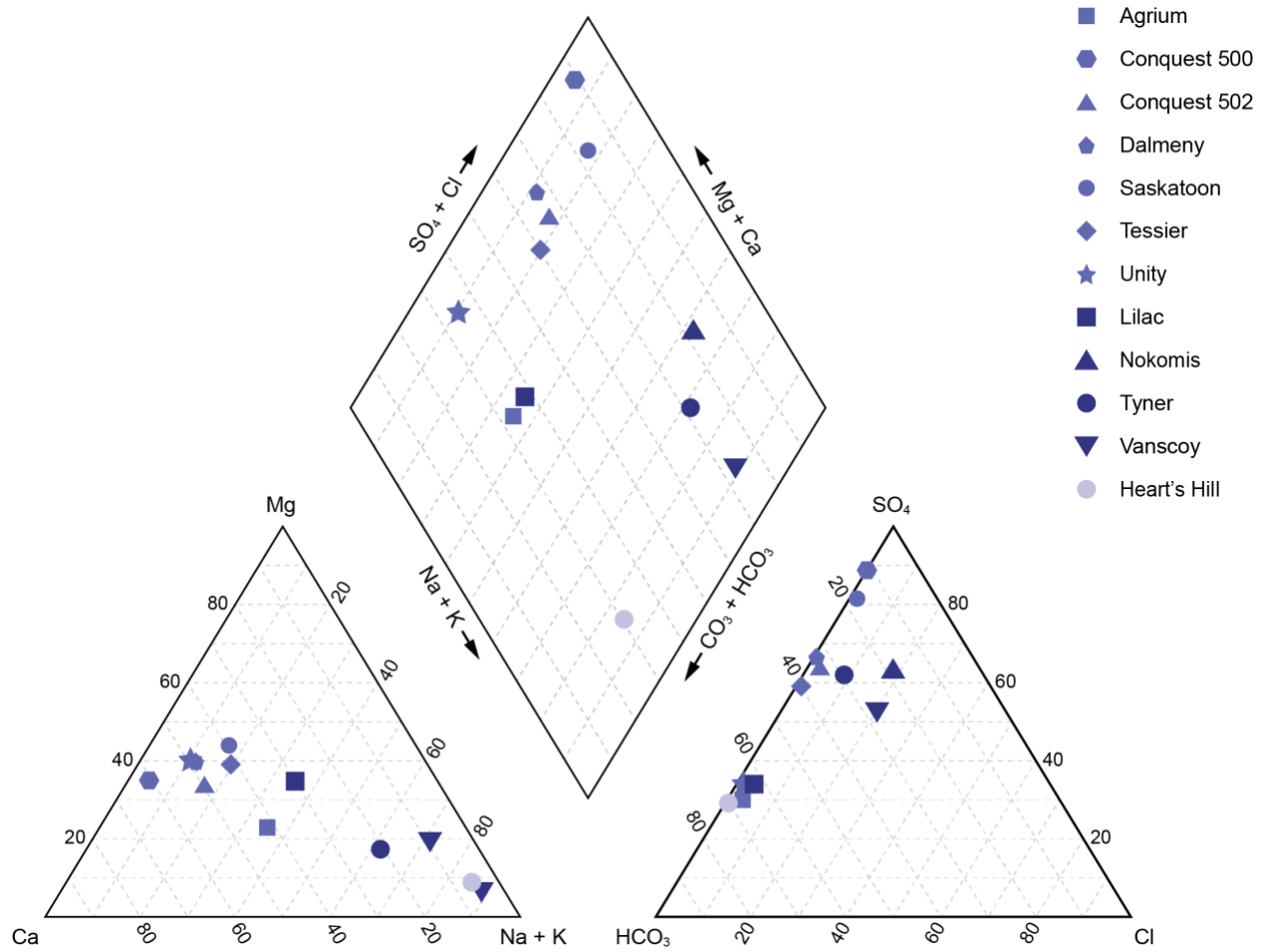
- 721 US EPA Region 1. 2017. Low stress (low flow) purging and sampling procedure for the
722 collection of ground water samples from monitoring wells. *EQASOP-GW4*, 30 p.
- 723 Wassenaar, L. I., and M. J. Hendry. 2000. Mechanisms controlling the distribution and transport
724 of ^{14}C in a clay-rich till aquitard. *Groundwater* 38, no. 3: 343–49.
- 725 Whitaker, S., and E. Christiansen. 1972. The Empress Group in southern Saskatchewan.
726 *Canadian Journal of Earth Sciences* 9, no. 4: 353–60.
- 727 Wick, K., C. Heumesser, and E. Schmid. 2012. Groundwater nitrate contamination: factors and
728 indicators. *Journal of environmental management* 111: 178–86.
- 729 Wolfe, S. A., J. Ollerhead, and O. B. Lian. 2002. Holocene eolian activity in south-central
730 Saskatchewan and the southern Canadian prairies. *Géographie physique et Quaternaire*
731 56, no. 2: 215–27.
- 732
- 733

734 **Figures**



735

736 **Figure 1:** Site map (a) showing sampled wells, aquifer type, and the approximate extent of buried
737 valley aquifer locations (buried valley aquifer shape file modified from Cummings et al. 2012)



742

743

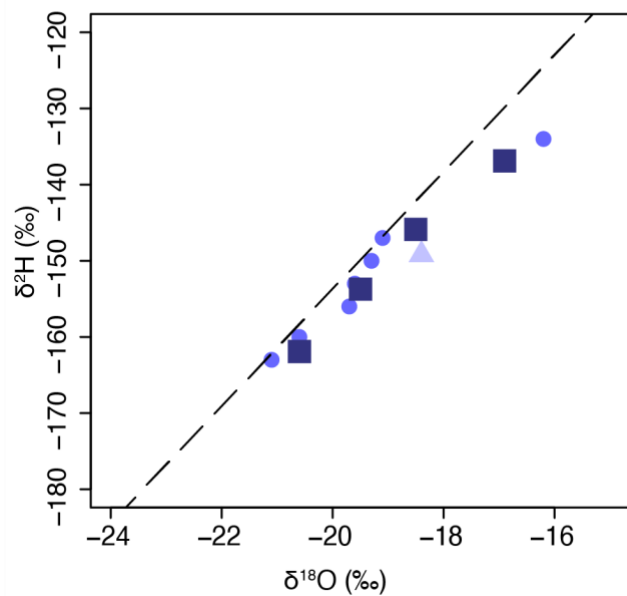
Figure 3: Piper plot showing the distribution of major ions in samples analyzed in this study.

744

Samples higher in Na and Cl tend to be buried valley samples, while intertill aquifers have a

745

range of dominant cations with very little Cl relative to HCO₃ and SO₄.

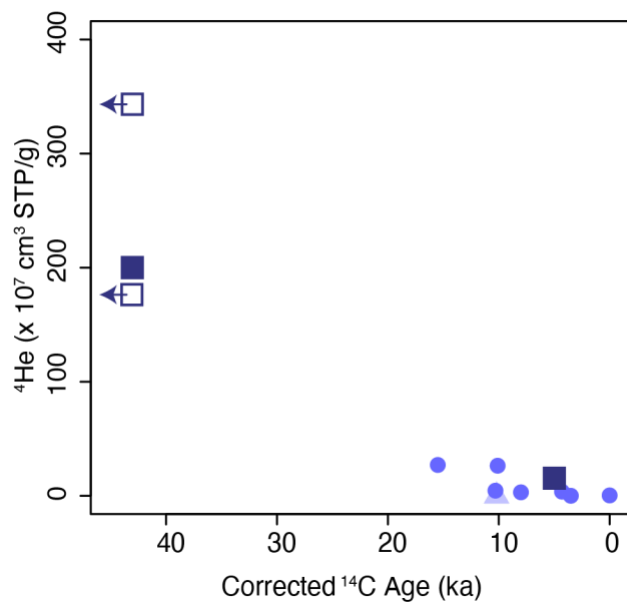


746

747 **Figure 4:** Stable water isotope values of intertill (*blue circles*), buried valley (*purple squares*),
748 and bedrock (*green triangle*) aquifers relative to the Local Meteoric Water Line (*dashed black*
749 *line*) (Koehler 2019).

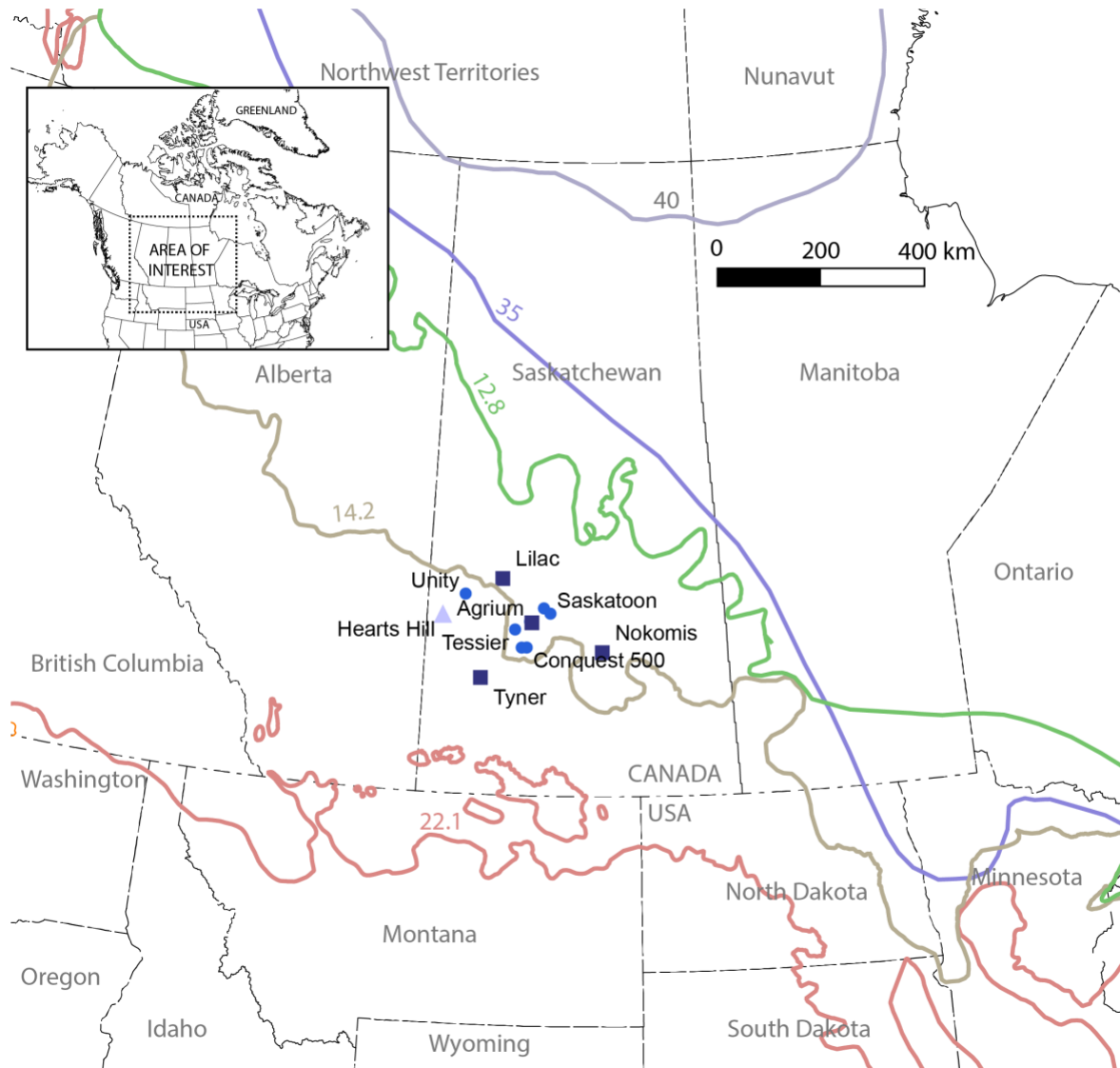
750

751



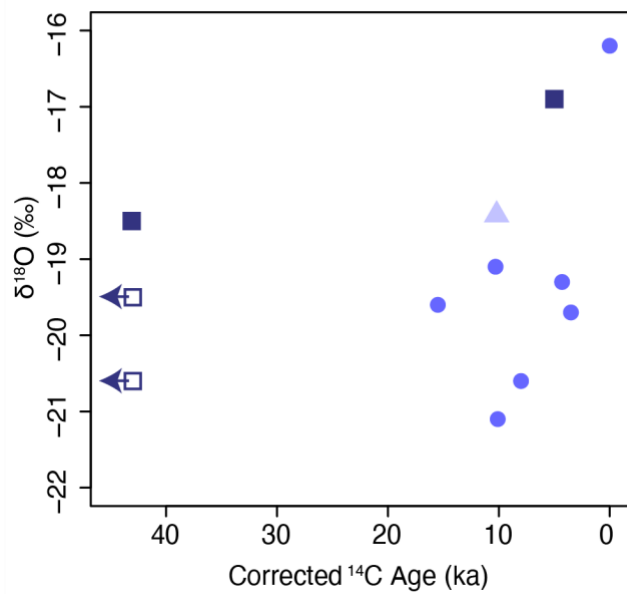
752

753 **Figure 5:** Air-corrected radiogenic ${}^4\text{He}$ ($\text{cm}^3 \text{ STP/g}$) versus corrected ${}^{14}\text{C}$ age (ka) of intertill (*blue*
 754 *circles*), buried valley (*purple squares*), and bedrock (*green triangle*) aquifers. Open purple
 755 squares indicate ${}^4\text{He}$ values for samples with no detectable radiocarbon.



756
757

758 **Figure 6:** Study area showing the southern extent of the Laurentide Ice Sheet (ages in ka)
 759 (Dalton et al. 2020, 2022). The region was glaciated during the LGM (i.e., 22.1 to 14.2 ka) for
 760 intertill (*blue circles*), buried valley (*purple squares*), and bedrock (*green triangle*) aquifers. The
 761 study area has been ice-free since at least 12.8 ka and prior to 30 ka back to at least 65 ka.



762

763 **Figure 7:** $\delta^{18}\text{O}$ values (‰) show no clear relation with corrected groundwater radiocarbon age
764 for intertill (*blue circles*), buried valley (*purple squares*), and bedrock (*green triangle*) aquifers.

765 Note: open purple squares indicate $\delta^{18}\text{O}$ values for samples with non-detect ^{14}C .